DEPARTMENT OF THE INTERIOR

U. S. GEOLOGICAL SURVEY

Seismic Responses for Circularly Symmetrical Bodies

By M. W. Lee[1]

Open-File Report 86-553

[1]U.S. Geological Survey, Box 25046, MS 960, Denver Federal Center, Denver, CO 80225

1986

TABLE OF CONTENTS

ILLUSTRATIONS

Seismic Responses for Circularly Symmetrical Bodies

By M. W. Lee

ABSTRACT

Diffraction responses of the acoustic wave equation for a circularly symmetrical body such as a circular disc or cone were formulated based on Trorey's (1977) method. An accurate numerical procedure is presented for the diffraction response of a circular disc model. However, an approximate solution is proposed for a circular cone model because of its non-plane surface.

This modeling technique was applied to the investigation of side echo problems encountered in the interpretation of multichannel seismic data over craters created by nuclear blasts at Enewetak Atoll in the Marshall Islands (Grow and others, 1986).

INTRODUCTION

Conventional multichannel seismic-reflection profiling techniques are based on an assumption of two-dimensional topography and structure. Reflections of topography or buried structures from outside the plane of the profile result in side echoes that cannot easily be corrected with presently available acquisition and processing techniques. Seismic data acquired over nuclear craters in Enewetak Atoll showed side echoes off the main reef, crater rims, and random pinnacle reefs; and these side-echoes presented difficult interpretational problems (Grow and others, 1986). This diffraction modeling study was initiated in order to illustrate the side echoes from the almost circularly symmetrical crater.

A general procedure of computing diffraction response using an acoustic wave equation can be found in Trorey (1970, 1977), Hilterman (1970), and Berryhill (1977). Some of the applications to the circularly symmetrical bodies are shown in Hilterman (1970, 1982).

In this investigation, Trorey's (1977) approach is adapted to generate acoustic responses for the circularly symmetrical bodies. In the case of a circular disc-type body, Trorey's formula provides an accurate numerical procedure, because the disc is a plane surface. However, Trorey's approach is very difficult to implement for a circular cone-type body, because a conical surface is not a plane surface. Thus, in this report, an approximate solution for the conical surface is presented. Combining this modeling method with an interpolation approach for circularly symmetrical bodies by Herman and others (1982) provided the necessary seismic responses for studying the effects of the side echoes present in the seismic data of Enewetak Atoll.

THEORY

The general diffraction theory for arbitrary source-receiver locations was developed by Trorey (1977) and Berryhill (1977) using an acoustic wave equation. In this paper, Trorey's formula was adapted in order to investigate the seismic response of a circularly symmetrical body such as a circular disc or cone.

Assume that a reflecting surface is a plane reflector located in the X-Y plane in a homogeneous half-space (fig. 1), the source and detector are located in the X-Z plane, and the reflection coefficient (r) is independent of the angle of incidence. Let $(0, 0, Z_d)$ be the coordinate of the

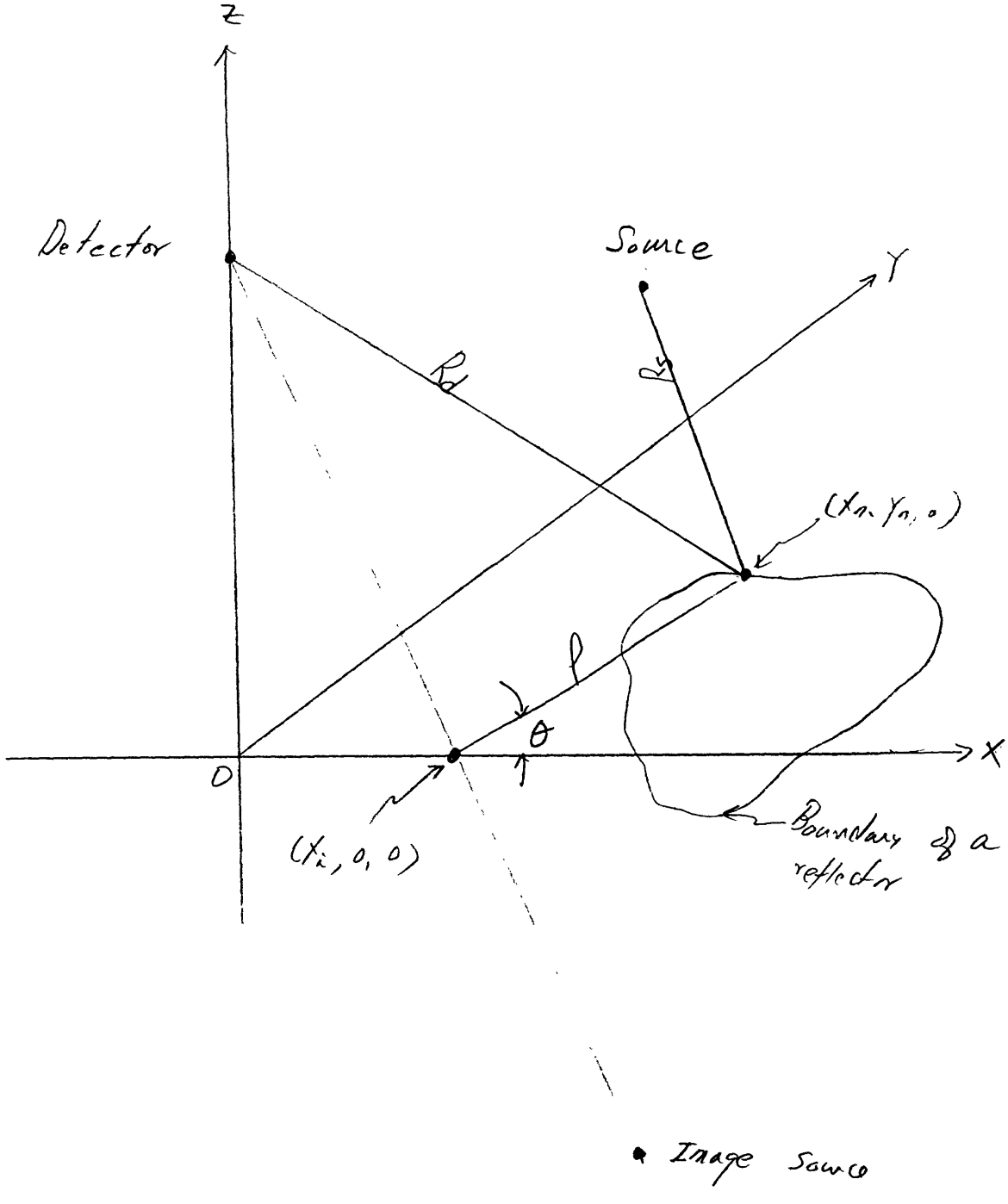

Figure 1.--Geometrical relation among source, receiver, and an elementary reflector in the X-Y plane. Detector is located in the Z-axis, and source is in the X-Z plane.

detector, $(X_s, 0, Z_s)$ be the coordinate of the source, and $(X_n, Y_n, 0)$ be the coordinate of the boundary of the reflecting surface. Then from Trorey (1977), the seismic response can be written as:

$$\phi(t) = \frac{r\delta(t-t_s)}{Vt_s}\varepsilon_s \pm \frac{r}{4\pi V}\oint_\theta b(t,\theta)\delta(t-t_d)\,d\theta \qquad (1)$$

$$\triangleq \phi_s(t) \pm \phi_d(t),$$

where

V: medium velocity,

t_s: specular reflection time,

t_d: traveltime from the source to the boundary of the reflector plus traveltime from the boundary to the detector (diffraction time),

and ε_s: equals 1 if the specular reflection exists, and 0 otherwise.

In equation (1), $\phi_s(t)$ represents the specular reflection response and $\phi_d(t)$ represents the diffraction response and $b(t, \theta)$ is given by:

$$b(t,\theta) = \frac{\rho\left(\frac{Z_d}{R_d} + \frac{Z_s}{R_s}\right)}{\left[\rho t - \frac{X_s(Z_d R_s - Z_s R_d)\cos\theta}{V(Z_s + Z_d)}\right]}, \qquad (2)$$

with

$$\rho^2 = (X_i - X_n)^2 + Y_n^2,$$

and

$$R_d^2 = (X_d - X_n)^2 + Y_n^2 + Z_d^2,$$

$$R_s^2 = (X_s - X_n)^2 + Y_n^2 + Z_s^2.$$

The upper sign in equation (1) is used for ε_s=0, and the lower sign for ε_s=1.

Utilizing a property of the delta function, the diffraction response in equation (1) can be written by the following equation:

$$\phi_d(t) = \frac{r}{4\pi V}\oint_\theta b(t,\theta)\,\delta\left[t - t_d(\theta)\right]d\theta \qquad (3)$$

$$= \frac{r}{4\pi V}\, b(t_d,\theta)\,\frac{d\theta}{dt_d}.$$

The main computational effort required for computing the diffraction response is the evaluation of $d\theta/dt_d$. This derivative term can be evaluated by:

$$\left(\frac{d\theta}{dt_d}\right)^{-1} = \frac{d}{d\theta}\left(\frac{R_s + R_d}{V}\right) = \frac{1}{V}\left(\frac{\partial R_s}{\partial X_n} + \frac{\partial R_d}{\partial X_n}\right)\frac{dX_n}{d\theta} . \tag{4}$$

In the case of a reflection surface being a circular disc with a radius "a", and the center of the disc being located at (X_c, 0, 0) (fig. 2a), then the boundary of the reflecting surfaces (X_n, Y_n, 0) as a function of θ can be derived as:

$$X_n = \frac{X_c + X_i \tan^2\theta \pm \sqrt{(X_c + X_i\tan^2\theta)^2 - \sec^2\theta\,(X_c^2 + X_i^2\tan^2\theta - a^2)}}{\sec^2\theta} \tag{5}$$

and

$$Y_n = \pm\sqrt{a^2 - (X_n - X_c)^2}$$

Also, the required derivative term $dX_n/d\theta$ in equation (4) is given by:

$$\frac{dX_n}{d\theta} = \sin 2\theta\left[X_i - X_c \mp \frac{a^2 + (X_c - X_i)^2\cos 2\theta}{2\cos\theta\sqrt{a^2 - (X_c - X_i)^2\sin^2\theta}}\right] \tag{6}$$

Utilizing equations (1) through (6), the seismic response of a circular disc for an arbitrary source and receiver combination can be evaluated. Of particular interest in this paper is the computation of the seismic response for the coincident source and receiver. By shifting the center of the disc to the origin of the coordinate (that is, X_c=0), the seismic diffraction response can be written as:

$$\phi_d = \frac{r}{4\pi V}\,\frac{Z_s}{X_s t_d}\left(\frac{dX_n}{d\theta}\right)^{-1} , \tag{7}$$

with

$$X_n = X_s\sin^2\theta \pm \sqrt{a^2\cos^2\theta - X_s^2\sin^2\theta\cos^2\theta} ,$$

$$t_d = \frac{2}{V}\sqrt{Z_s^2 + X_s^2 + a^2 - 2X_n X_s} ,$$

and

$$\frac{dX_n}{d\theta} = \sin 2\theta\left[X_s \mp \frac{a^2 + X_s^2\cos 2\theta}{2\cos\theta\sqrt{a^2 - X_s^2\sin^2\theta}}\right] .$$

The sign convention in equation (7) is:

a) When $0<X_s<a$,

the upper sign: $0<\theta<\pi/2$ or $3\pi/2 <\theta<2\pi$;

the lower sign: otherwise.

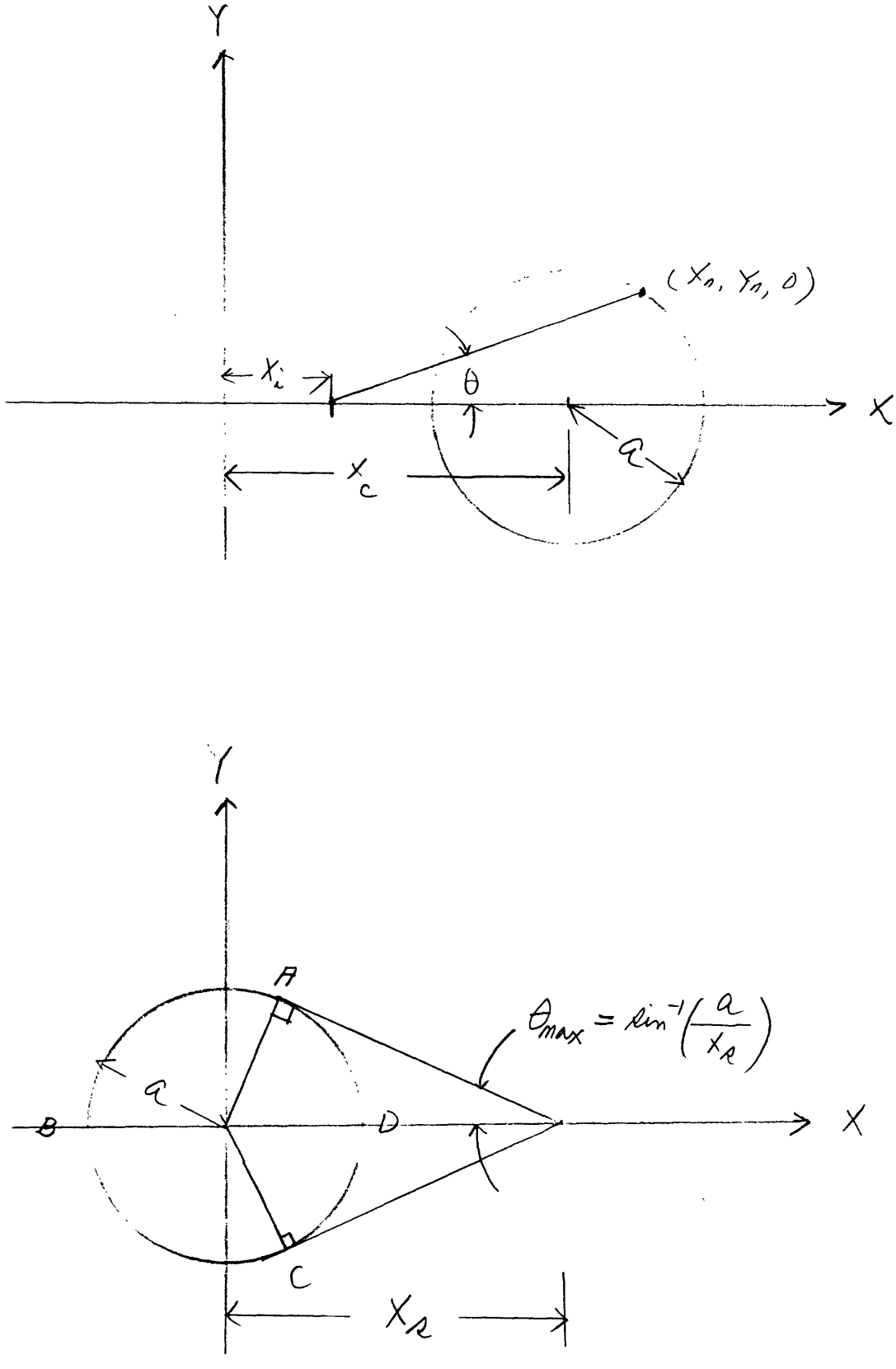

Figure 2.--Geometrical relationship of a circular disk model pertinent to Equation 5. a) Center of a disk is (X_c0); b) center of a disk is (0, 0).

b) When $X_s > a$,

the upper sign: X_n is an arc ADC in figure 2b;

the lower sign: X_n is an arc ABC in figure 2b.

In figure 2, θ_{max} is given by:

$$\theta_{max} = \sin^{-1}\left(\frac{a}{|X_d|}\right)$$

The solution in equation (7) does not exist when $X_s=0$. In this case, the solution can be easily obtained directly from equation (1), simply because t_d is not a function of θ. Thus, the solution is given by:

$$\begin{aligned} \phi_d &= \frac{r}{4\pi V} \oint_\theta b(t,\theta)\,\delta(t-t_d)\,d\theta, \\ &= \frac{r}{2}\,\frac{Z_d}{R_d^2}\,\delta\left(t-\frac{2R_d}{V}\right). \end{aligned} \tag{8}$$

The diffraction response from a conical surface cannot be evaluated by equation (1), because the conical surface is not a plane surface. Conceptually, in this situation, Hilterman's approach (1970) could be more suitable than Trorey's, even though Hilterman's approach requires a complicated numerical integration. Thus in this paper, an approximate method is proposed. The validity of this method or approximation can be tested by a physical modeling technique:

Figure 3 shows a conical surface. The proposed approximation is that the non-plane angle $\emptyset$ in figure 3 is substituted into equation (1) as a plane angle and a curvature effect derived by Hilterman (1975) is included. In other words,

$$\begin{aligned} \phi_d &\cong \frac{C_e r}{4\pi V} \oint_\phi b(t,\phi)\,\delta\left[t-t_d(\phi)\right]d\phi, \\ &= \frac{C_e r}{4\pi V}\, b(t_d,\phi)\,\frac{d\phi}{dt_d}, \end{aligned} \tag{9}$$

where C_e is the curvature effect. The curvature effect C_e is given by (Hilterman, 1975):

$$C_e = \sqrt{\left(\frac{1}{1+R_0/R_1}\right)\left(\frac{1}{1+R_0/R_2}\right)}, \tag{10}$$

where

R_0: normal incident path length (or wavefront radius);

R_1, R_2: two principal radii of curvature of the reflector. This curvature effect should be applied to the specular reflections also.

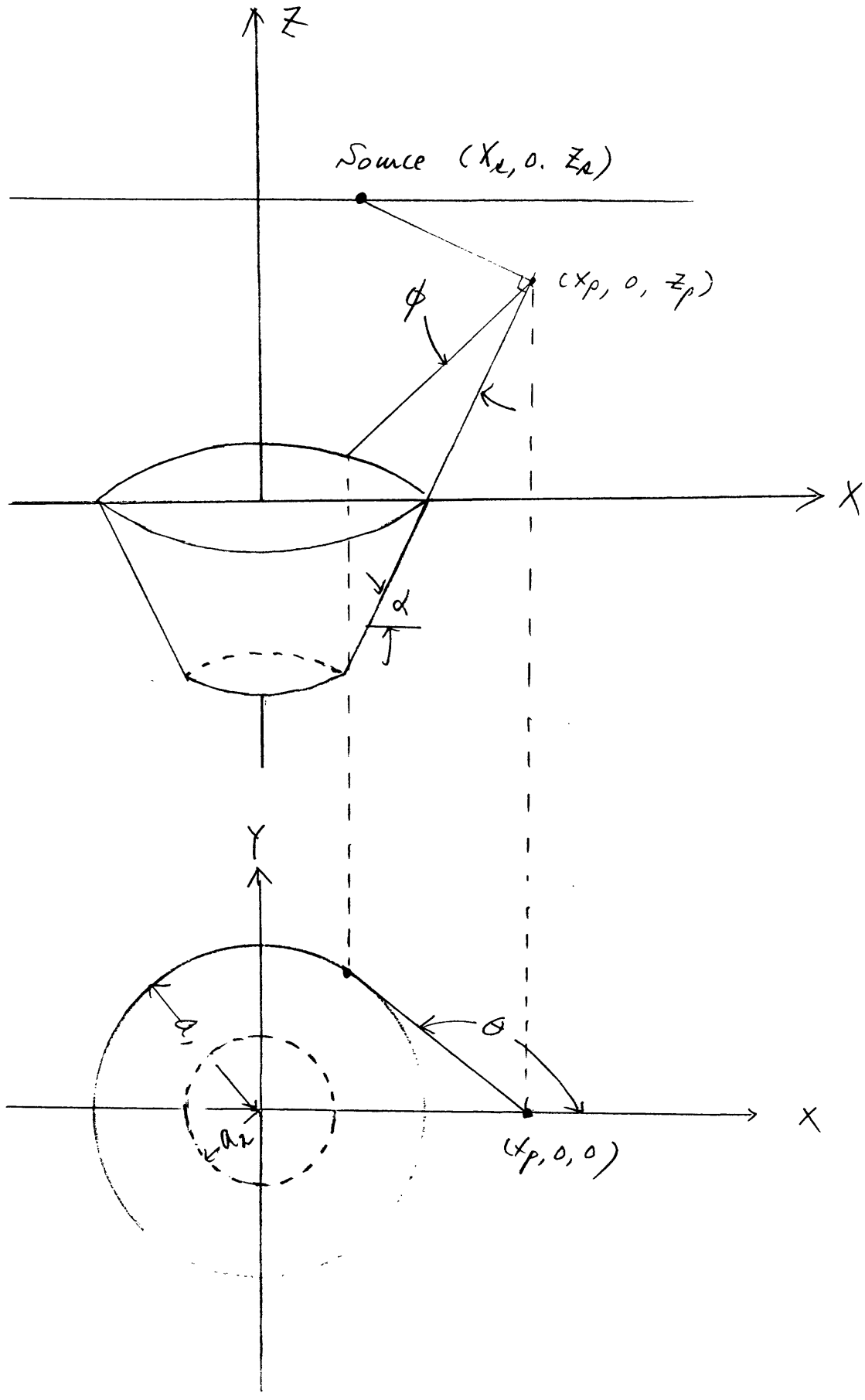

Figure 3.--Geometrical relationship of a circular cone model. a) Side view; b) plan view.

Using figure 3, $d\phi/dt_d$ can be computed by $d\theta/dt_d$, where θ is a true plane angle, and the solution (9) can be written by the following formulae (see appendix):

$$\phi_d \cong \frac{C_e r}{4\pi} \frac{\tilde{Z}}{2R_2 Z_2} \frac{A}{D_1 \sin\phi}, \tag{11}$$

where

$$A = \frac{Q_1 Q_2 \sin\theta}{D_2} \left(\frac{dX_n}{d\theta}\right)^{-1} + \frac{Q_1 X_p}{Q_2 D_2} \cos\theta - \left(Z_p^2 + Q_1 Q_2 \cos\theta\right) \frac{X_p}{D_2^3},$$

$$\phi = \cos^{-1}\left[\frac{Z_p^2 + Q_1 Q_2 \cos\theta}{D_1 D_2}\right],$$

$$\tilde{Z}^2 = (Z_2 - Z_p)^2 + (X_p - X_2)^2,$$

$$Q_1^2 = (X_p - a)^2, \quad Q_2^2 = (X_p - X_n)^2 + Y_n^2,$$

$$D_1^2 = Z_p^2 + Q_1^2, \quad D_2^2 = Z_p^2 + Q_2^2.$$

When $\alpha \to 0$, then:

$$X_p \to X_2, \quad Z_p \to 0, \quad \cos\phi \to \cos\theta, \text{ and } C_e \to 1.$$

Thus,

$$\lim_{\alpha \to 0} A \to Q_1 \sin\phi \left(\frac{dX_n}{d\theta}\right)^{-1}.$$

Therefore,

$$\lim_{\alpha \to 0} \phi_d \to \frac{r}{4\pi} \frac{Z_2}{2R_2 X_2} \frac{Q_1 \sin\phi}{D_1 \sin\phi} \left(\frac{dX_n}{d\theta}\right)^{-1},$$

$$= \frac{r}{4\pi V} \frac{Z_2}{X_2 t_d} \left(\frac{dX_n}{d\theta}\right)^{-1}. \tag{12}$$

Equation (12) is identical to equation (7), which is an exact solution. This implies that when α is small, the approximate solution (11) is very reliable. It can also be established that when "a" is large, the solution (11) approaches the exact solution, because the conical surface approaches the plane surface as "a" becomes larger.

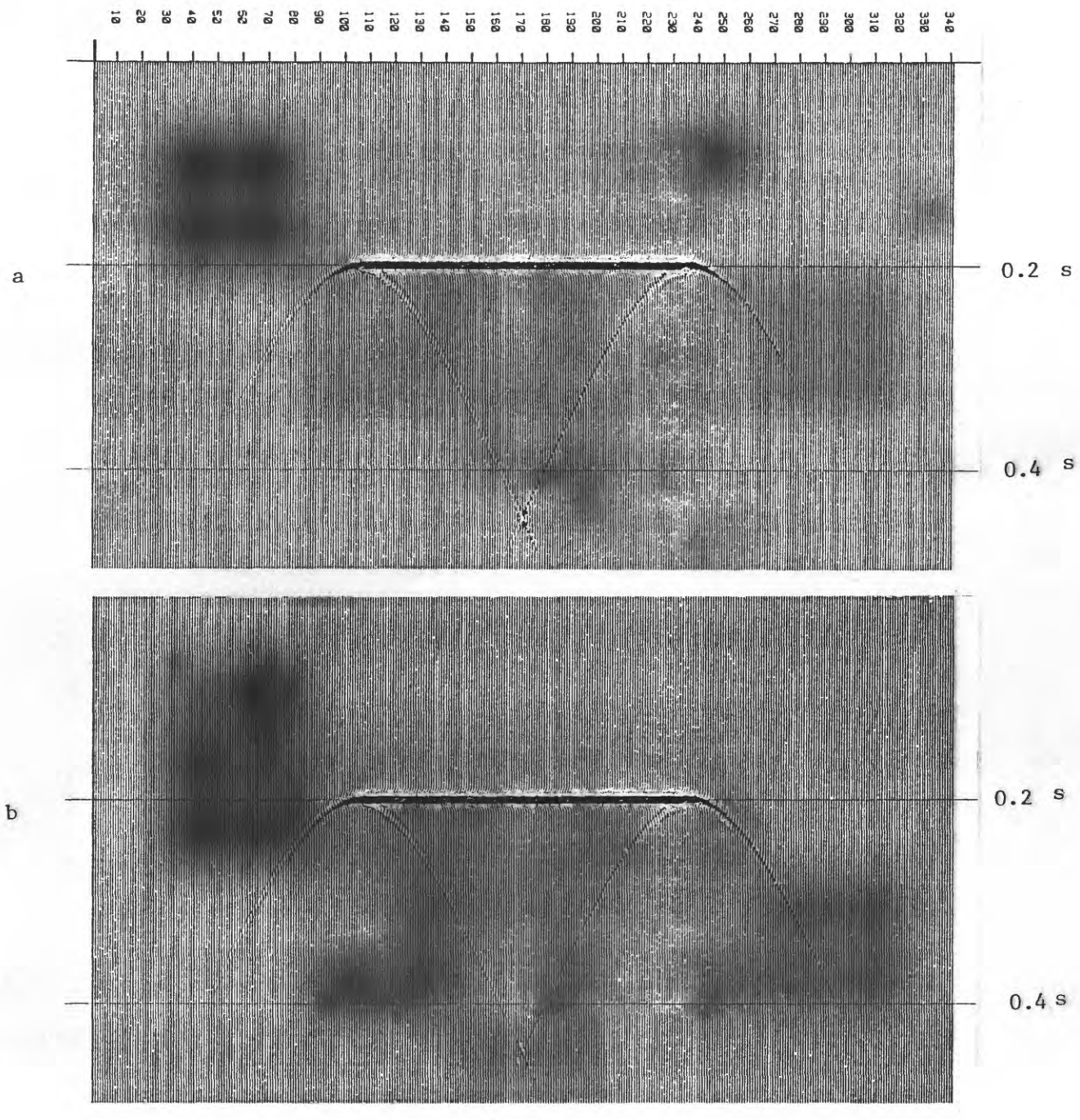

Figure 4.--Seismic response for a circular disk. a) 2-dimension plate model; b) 3-dimension disk model.

EXAMPLES

For all the synthetic sections, the geometrical spreading loss of acoustic energy is compensated for, and the reflection coefficients of all layers are assumed to be identical. The term "equivalent two-dimensional model" means that the cross-section of the two-dimensional model is identical to that of the circularly symmetrical model, while the other dimension is infinitely long. For example, the equivalent two-dimensional model of a circular disc is an infinitely long plate.

Disc Model

Figure 4a shows the seismic response of a single circular disc with a radius of 200 m at the depth of 100 m. The medium velocity used for the model is 1 km/s and 80 Hz symmetrical Ricker wavelet is considered to be an input wavelet. Figure 4b shows the seismic response of an equivalent 2-dimensional model. The strong diffraction at the center of the disc in figure 4a is the result from the focused diffraction at the edges of the disc. This focused diffraction, which can be obtained from equation (8), is the unique seismic response for the circularly symmetrical bodies. Lee (1984) investigated the amplitude variation of this focused diffraction with respect to the size of a disc and the source-receiver distance and demonstrated that the amplitude variation with respect to the size of the disk is similar to the amplitude variation with respect to a bed thickness.

The polarity of the diffraction events outside the disc has the same polarity as the reflection event, while the polarity under the disc has a polarity opposite to the reflection. The polarity of the diffracted event for a disc model is identical to the 2-dimensional model. However, the circular disc model contains more diffracted energy under the disc than outside of the disc. The strong diffracted energy under the disc is the main difference between 2-dimensional plate and 3-dimensional disc models.

Mound Model

The seismic response and geometry of the 3-dimensional mound model is shown in figure 5. Figure 6 shows the response of the equivalent 2-dimensional Horst model. The medium velocity of this model is 1 km/s, the depth of the top of the mound is 50 m, and 80 Hz Ricker wavelet was used. In order to clarify the diffracted events for the conical surface of the mound, only the specular reflection response is shown in figure 7a, and figure 7b shows only the diffracted events.

Thus, the combination of figures 7a and 7b will result in figure 6. The specular reflection amplitude originated from the conical surface (A-B in figure 7) is very small compared to the other flat reflection amplitude. This amplitude reduction is the result of curvature effect on the conical surface and is shown in equation (10).

The diffracted events originated at B in figure 7b (or top of the mound) have different characteristics compared to the results shown in figure 4. The large amplitude diffracted event off B is the result of the constructive interference of the two diffraction tails, one from the top disc surface and the other from the conical surface.

Figure 5 clearly shows two focused diffracted events, one from the top of the structure and the other from the rim of the lower surface. One noticeable difference between 2- and 3-dimensional modeling shown in figures 5 and 6 is that the 2-dimensional model has a long diffraction tail under the structural high, while the 3-dimensional model has focused diffractions.

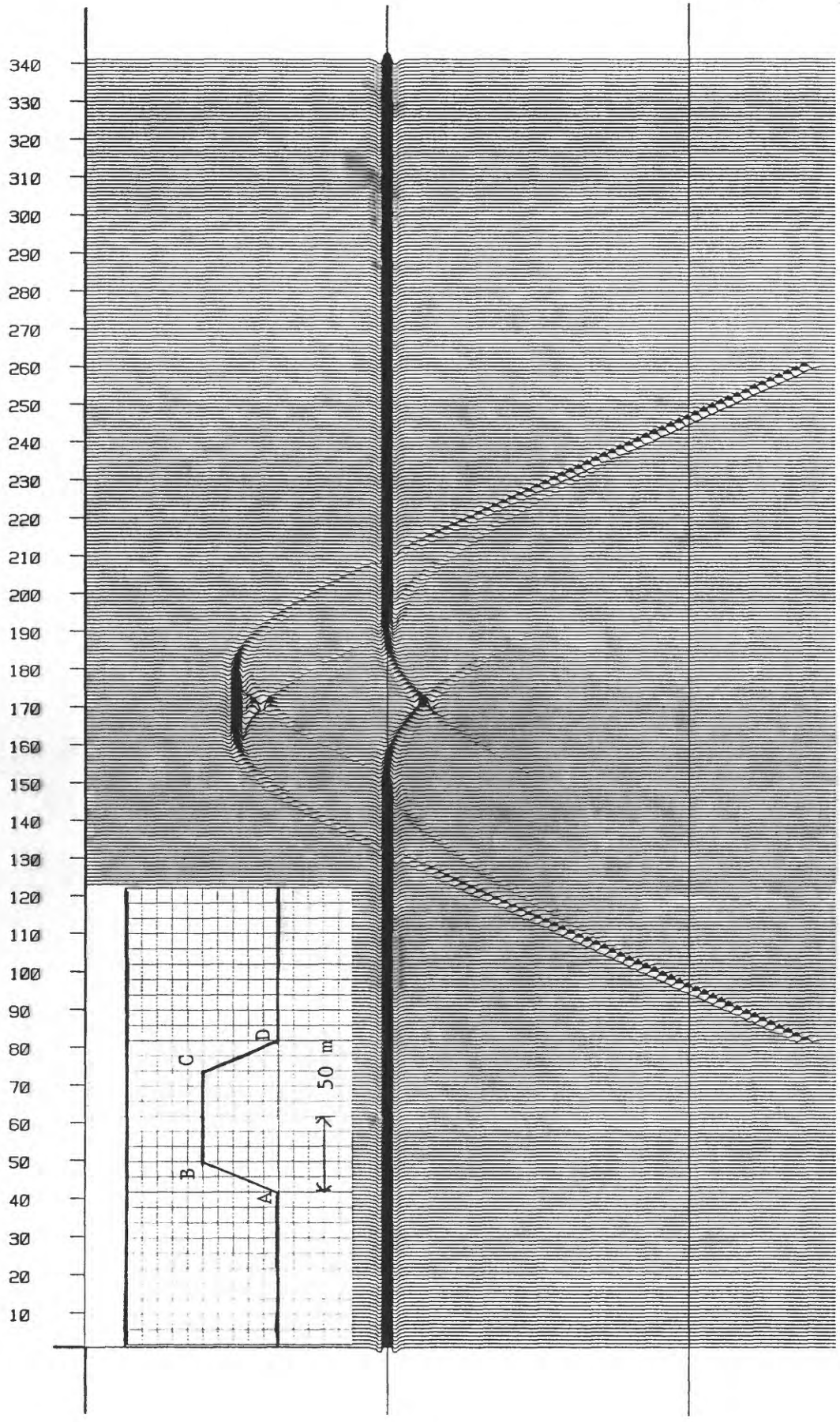

Figure 5.--Seismic response for a 3-dimensional mound model.

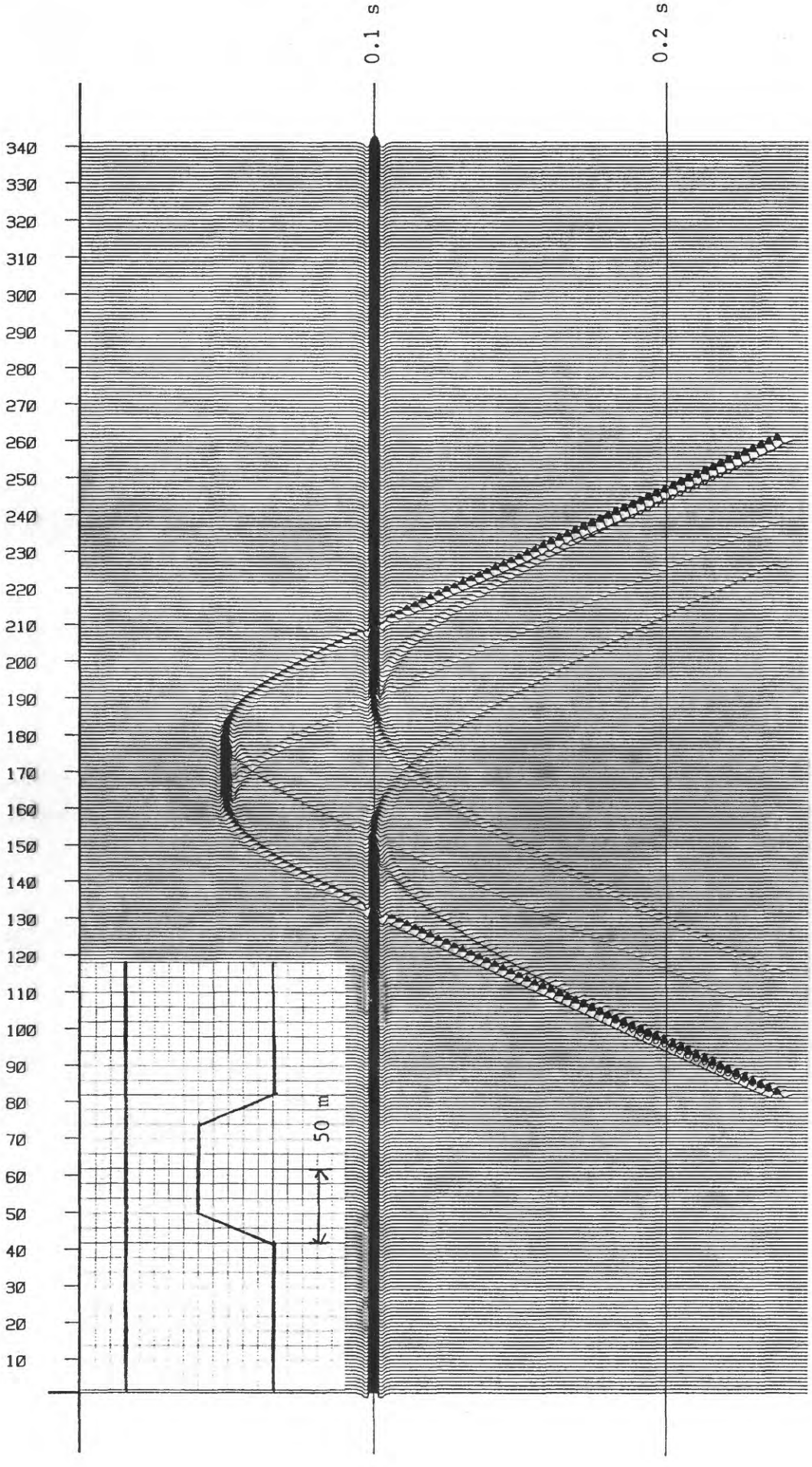

Figure 6.--Seismic response for a 2-dimensional horst model.

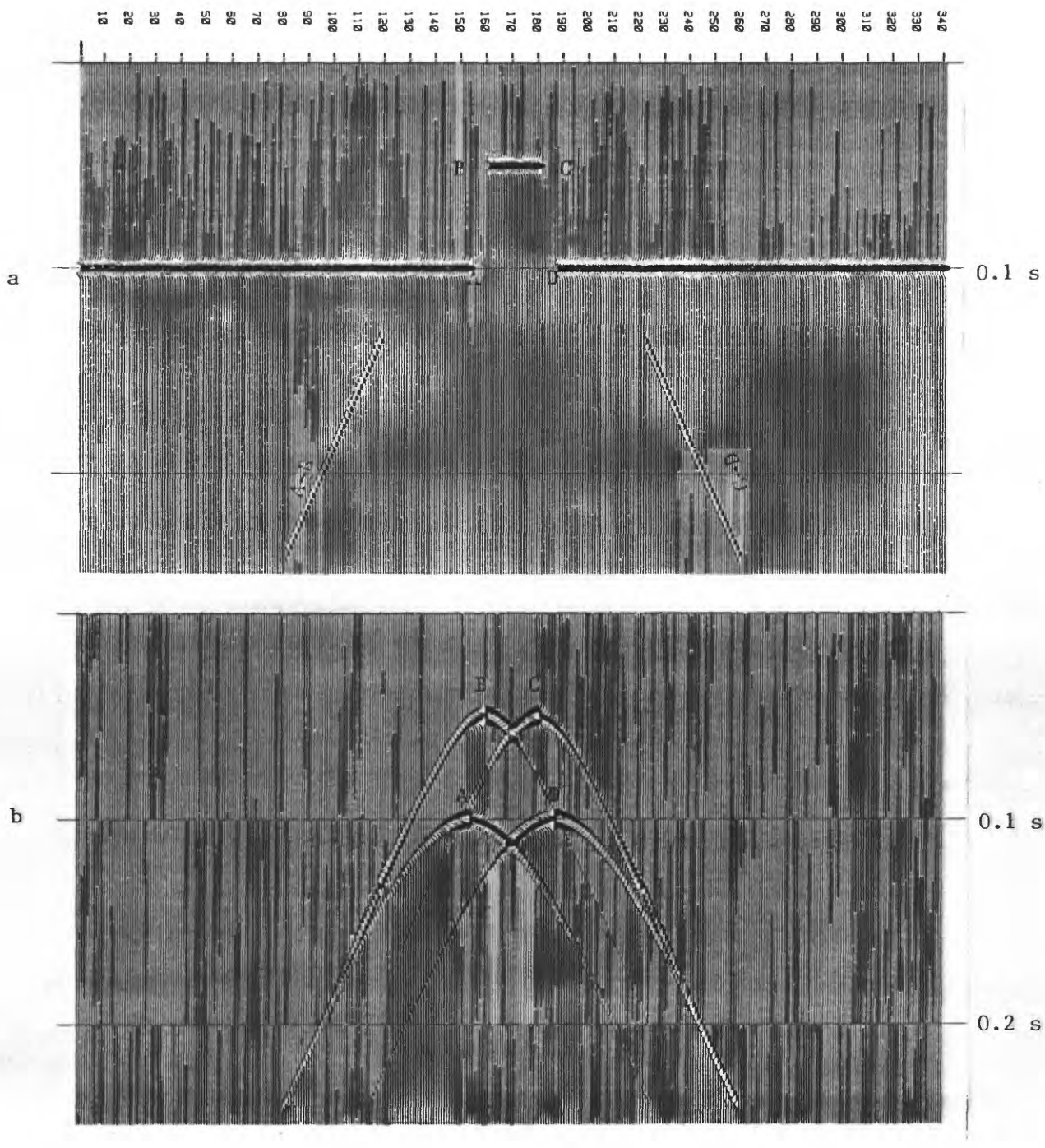

Figure 7.--Decomposition of a seismic response shown in figure 5.
a) Specular reflectors; b) diffractions.

As mentioned in the theory section, results of this model are an approximation. However, by comparing the results of the 2-dimensional horst model, the seismic response of the circular mound model appears at least qualitatively reasonable. Similar seismic response and comparison shown in figures 5 and 6 can be found in Hilterman (1970), where he compared the 3-dimensional dome model with an equivalent 2-dimensional anticlinal model.

APPLICATION TO THE SIDE-ECHO PROBLEM

Figure 8 shows two seismic lines A and B, where line A passes the center of the body and line B is the offset line. Herman and others (1982) present an easy method in computing seismic response for the offset seismic lines by an interpolation method when the seismic responses for the zero-offset line is known. This method can be illustrated easily by using figure 8. For example, the seismic response at point L_B on line B is exactly the same as the seismic response at point L_A on line A. Using an interpolation method, we can project the seismic response on line B using the data on line A.

In the following example, the seismic response for the zero-ofset section was derived by the formula derived in this article. Seismic sections for the off-set line were computed by the interpolation method of Herman and others (1982).

As mentioned in the introduction, the seismic lines acquired at Enewetak Atoll were contaminated by many side echoes from the main reef, crater rims, and many pinnacle reefs. While the reflection profiles cannot be corrected for these effects, computer models using simplified topography illustrate these problems. For instance, a circular model of OAK crater with an inner crater and an intermediate terrace (fig. 9A) illustrates the side-echo and diffraction effects that complicate the interpretation of the multichannel seismic data from Enewetak.

The model's first layer models the sea floor of the apparent crater. The second layer simulates a shallow-subsurface reflector which is truncated beneath the inner crater. The third layer represents a deep reflector which is down-dropped beneath the inner crater. The impulse-like strong seismic response under the center of the model (fig. 9B) results from the focused diffractions from the edges of the discontinuous subsurface layer. Numerous diffraction tails, some originating from the topographic relief of the apparent crater and others from the truncational edge of the second layer, can be clearly observed under the crater. This diffraction effect is a major side-echo problem in interpreting seismic data.

Figure 9C shows the seismic response when the seismic line is offset 35 m from the center of the crater. Notice the synclinal appearance of the diffraction tails under the crater. When the line-offset distance is 75 m (fig. 9D), the truncated second layer appears as a continuous reflector, and the water-bottom reflection reveals a very complicated interference pattern. The seismic responses of the deep crater have a synclinal appearance. Similar side-echo problems due to the 3-dimensional topographic and subsurface effects mentioned above were observed in multichannel seismic data from Enewetak Atoll.

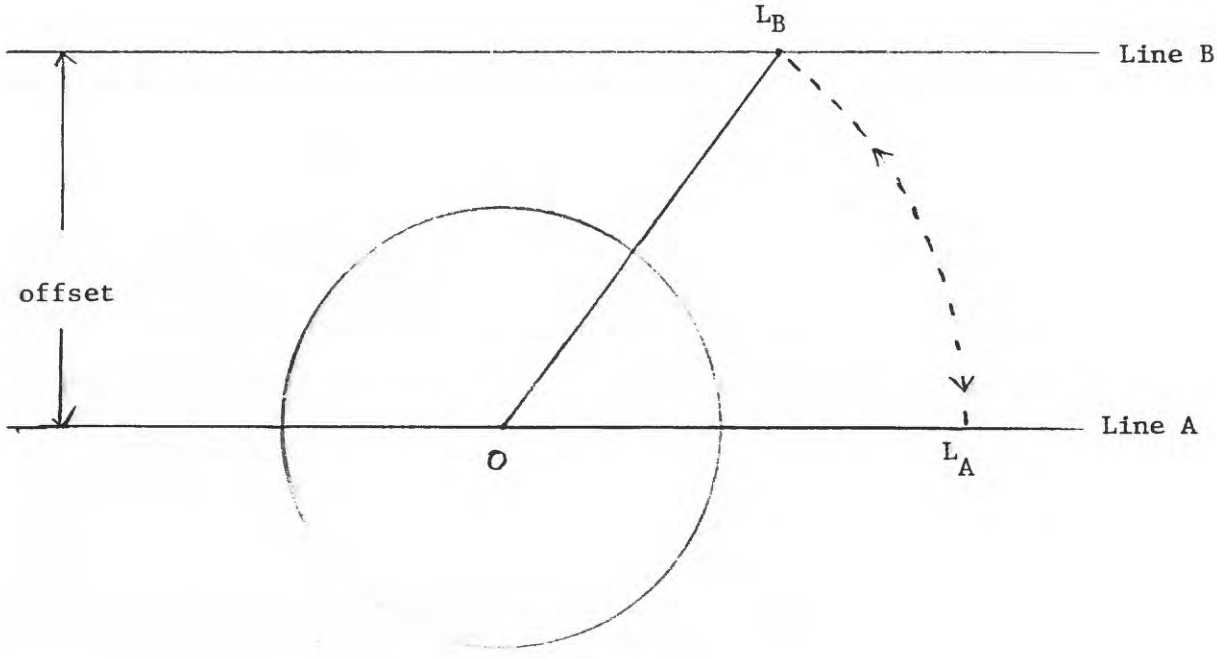

Figure 8.--Relationship showing a circularly symmetrical body and seismic lines.

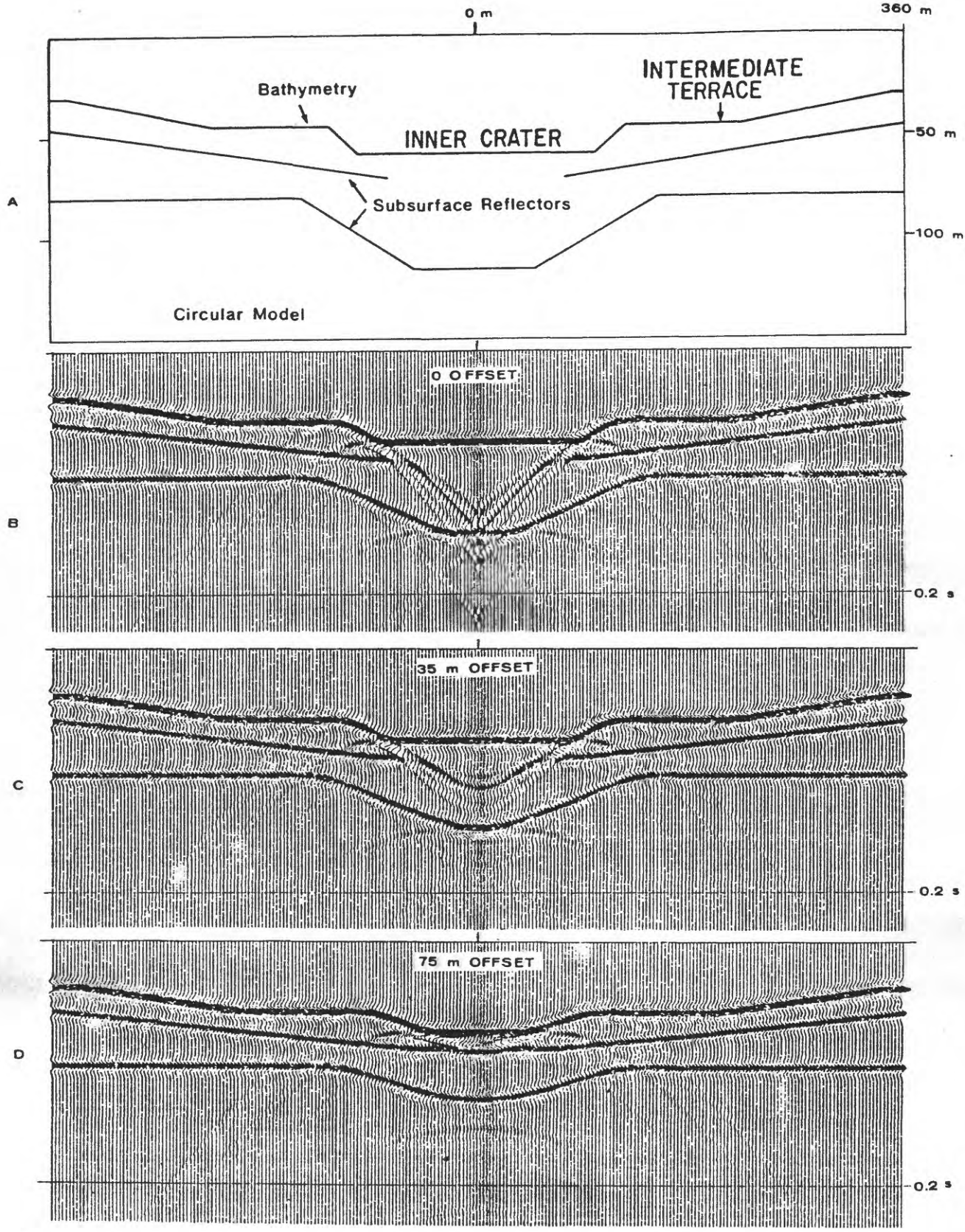

Figure 9.--Three-dimensional circular crater model. a) Cross-section of model; b) modeled reflectors at 0 offset; c) modeled reflectors at 35 m; d) modeled reflectors at 75 m (from Grow and others, 1986).

CONCLUSIONS

A method for computing the diffraction response for a circularly symmetrical body is presented. An approximate solution for the conical surface including the curvature effect of the non-plane surface appears to be reasonable. This modeling technique in conjunction with the interpolation approach for circularly symmetrical bodies provided a means to evaluate the major side-echo problems in interpreting the multichannel seismic data over nuclear craters at Enewetak Atoll.

REFERENCES

Berryhill, J.R., 1977, Diffraction response for nonzero separation of source and receiver: Geophysics, v. 42, p. 1158-1176.

Grow, J.A., Lee, M.W., Miller, J.J., Agena, W.F., Hampson, J.C., Hester, D.S., and Woellner, R.A., 1986, Multichannel seismic-reflection survey of KOA and OAK craters, in Folger, D.S., Sea-floor observations and subbottom seismic characteristics of OAK and KOA craters, Enewetak Atoll, Marshall Islands: U.S. Geological Survey Bulletin 1678, p. D1-D46.

Herman, A.J., Anania, R.M., Chun, J.H., Jacewitz, C.A., and Pepper, R.E.F., 1982, A fast three-dimensional modeling technique and fundamentals of three-dimensional frequency-domain migration: Geophysics, v. 47, p. 1627-1644.

Hilterman, F.J., 1970, Three-dimensional seismic modeling: Geophysics, v. 35, p. 1020-1037.

Hilterman, F.J., 1975, Amplitude of seismic waves--A quick look: Geophysics, v. 40, p. 745-762.

Hilterman, F.J., 1982, Interpretative lessons from three-dimensional modeling: Geophysics, v. 47, p. 784-808.

Lee, M.W., 1984, Delineation of lenticular-type sand bodies by the vertical seismic profiling method: U.S. Geological Survey Open-File Report 84-265, 88 p.

Trorey, A.W., 1970, A simple theory for seismic diffraction: Geophysics, v. 35, p. 762-784.

Trorey, A.W., 1977, Diffractions for arbitrary source-receiver locations: Geophysics, v. 42, p. 1177-1182.

APPENDIX

Derivative of Equation 11

The integral with respect to ϕ in equation (9) for the conical surface should be performed along both the upper and lower circles. For convenience, the derivative of equation (11) is made along the upper circle. Let $(X_p, 0, Z_p)$ be the minimum traveltime coordinate from the source to the conical surface or the extension of it as shown in figure 3.

Then, from equation (2) $b(t_d, \phi)$ can be written as:

$$b(t_d, \phi) = \frac{z\sqrt{(x_p - x_s)^2 + (z_s - z_p)^2}}{t_d R_s} = \frac{V\tilde{z}}{R_s^2} .$$

Therefore, equation (10) can be written as:

$$\phi_d \cong \frac{c_e r}{4\pi V} \frac{\tilde{z} V}{R_s^2} \left| \frac{d\phi}{dt_d} \right| = \frac{c_e r}{4\pi V} \frac{\tilde{z}}{R_s^2} \left| \left(\frac{2 dR_s}{V d\phi} \right)^{-1} \right| \qquad \text{(A-1)}$$

$$= \frac{c_e r}{4\pi} \frac{\tilde{z}}{2R_s Z_s} \left(\frac{d\phi}{d\theta} \right) \left| \left(\frac{dX_n}{d\theta} \right)^{-1} \right| .$$

Because $dX_n/d\theta$ is given in equation (7b), only $d\phi/d\theta$ is needed to evaluate equation A-1. Using the following relation between ϕ and θ,

$$\cos\phi = \frac{z_p^2 + Q_1 Q_2 \cos\theta}{D_1 D_2} \qquad \text{(A-2)}$$

$d\phi/d\theta$ can be derived.

By differentiating A-2 and rearranging the terms, the following can be shown:

$$D_1 \sin\phi \frac{d\phi}{d\theta} = \left[\frac{Q_1 Q_2 \sin\theta}{D_2} \left(\frac{dX_n}{d\theta} \right)^{-1} + \frac{X_p Q_1 \cos\theta}{D_2 Q_2} - \right.$$

$$\left. \frac{z_p^2 + Q_1 Q_2 \cos\theta}{D_2^2} \frac{X_n}{} \right] \frac{dX_n}{d\theta} \triangleq A \frac{dX_n}{d\theta} . \qquad \text{(A-3)}$$

Thus, combining A-1 and A-3:

$$\phi_d \cong \frac{c_e r}{4\pi} \frac{\tilde{z}}{2R_s X_s} \frac{A}{D_1 \sin\phi} .$$